J Fluoresc (2013) 23:947–955
DOI 10.1007/s10895-013-1220-z

ORIGINAL PAPER

Time-Resolved Flavin Adenine Dinucleotide Fluorescence Study of the Interaction Between Immobilized Glucose Oxidase and Glucose

Rosario Esposito · Ines Delfino · Maria Lepore

Received: 25 January 2013 / Accepted: 1 April 2013 / Published online: 11 April 2013

Abstract Time-resolved fluorescence experiments have shown that flavin adenine dinucleotide (FAD) fluorescence emission of sol–gel immobilized glucose oxidase (GOD) exhibits a three-exponential decaying behaviour characterized by long- (about 2.0–3.0 ns), intermediate- (about 300 ps) and short- (less than 10 ps) lifetime, each one being characteristic of a peculiar conformational state of the FAD structure. In the present work time-resolved fluorescence is used to monitor FAD signals in the time interval immediately following the addition of glucose at various concentrations in order to detect the conformational changes occurring during the interaction between sol–gel immobilized GOD and glucose. The analysis of time-dependent fluorescence emission signal has shown that the FAD conformational state changes during the process from a configuration with a prevalence of the state characterized by the long lifetime to a configuration with increased contribution from the process with the intermediate lifetime. The time needed to complete this configuration change decreases with the concentration of added glucose. The results here reported indicate that time-resoled fluorescence can be extremely useful for a better understanding of solid phase biocatalysis that is particularly important in light of their clinical and biotechnological applications.

Keywords Glucose oxidase · Glucose · Time-resolved fluorescence · FAD · Conformational changes

R. Esposito
Dipartimento di Scienze Fisiche, Università di Napoli "Federico II", Napoli, Italy

I. Delfino (✉)
Dipartimento di Scienze Ecologiche e Biologiche, Università della Tuscia, Viterbo, Italy
e-mail: delfino@unitus.it

M. Lepore
Dipartimento di Medicina Sperimentale, Seconda Università di Napoli, Napoli, Italy

Abbreviations

FAD	Flavin adenine dinucleotide
GOD	Glucose oxidase
ET	Electron transfer
TMOS	Tetramethoxysilane
TCSPC	Time-correlated single-photon counting
IRF	Instrument response function

Introduction

To delineate methods and devices for improving the capability of glucose testing and determination is a task that has attracted a significant research interest and development efforts over the past 20 years. Several approaches based on the study of the effects of the interaction between glucose oxidase (GOD) and glucose by different techniques have been proposed and tested [1–5]. Among these fluorescence-based methods have received great attention [6, 7], encouraged by both the special advantages of fluorescence methods for studying biological systems and the intrinsic GOD fluorescence emission [8, 9]. Very recently time-resolved fluorescence has been also proposed [10]. In fact, dynamical changes of GOD visible fluorescence are shown when oxidative processes are induced by means of glucose interaction [8, 9]. GOD is a homo-dimer molecule composed of two identical 80-kDa subunits and two non-covalently bound flavin adenine dinucleotide (FAD) complexes and catalyses the oxidation of glucose to gluconic acid through the reaction:

$$\mathrm{D-glucose} + \mathrm{O_2} \xrightarrow{\mathrm{GOD}} \mathrm{D-gluconolactone} + \mathrm{H_2O_2}$$
$$\mathrm{D-gluconolactone} + \mathrm{H_2O_2} \rightarrow \mathrm{d-gluconic\ \ acid}$$

The well-known reaction mechanism is the following: glucose reduces FAD to $FADH_2$ with formation of gluconolactone, which is rapidly hydrolysed to gluconic acid. At this point the dissolved oxygen reoxidises $FADH_2$ and produces H_2O_2. According to this cyclic scheme two species

display the fluorescence of FAD and $FADH_2$. The FAD structure is composed by flavoprotein and adenine dinucleotide (Fig. 1). FAD was extensively studied by using various methods, including Fourier-Trasform InfraRed and Ultra-Violet Raman spectroscopy and Nuclear Magnetic Resonance [7, 11–14]. The isoalloxazine (ISO) ring is responsible for the light emission of FAD in the visible spectral range and is linked with adenine through hydrogen-bonding. It was proposed that FAD exists in two conformations: an extended, open conformation, and a closed one, in which the ISO and adenine rings interact through a stacked conformation. The open conformation gives rise to the fluorescent component of FAD with a lifetime of about 2.8 ns, whereas a much faster fluorescence decay (lifetime about 4 ps) takes place as a consequence of the photoinduced electron transfer (ET) between adenine and flavin [15, 16]. The conformational changes experienced by the molecule during the lifetime of the excited states accounts for an intermediate lifetime component of about 0.3 ns. With femtosecond resolution, the fluorescence quenching of GOD due to ET with aromatic residues has been investigated and two decay constants of 1.8 ps and 10 ps have been measured [17]. Accordingly, three ranges for fluorescence lifetimes in flavins can be assumed to characterize the decay: long (τ_L about 2.0–3.0 ns), intermediate (τ_I about 300 ps) and short ($\tau_S \leq 10$ ps) lifetime, that can be ascribed to the open, intermediate and closed configuration, respectively. Recently, a time-resolved fluorescence study of the dynamical changes of FAD fluorescence occurring during the enzymatic reaction of GOD with glucose has allowed us to confirm that the GOD fluorescence decay curves are well-described by a three-exponential model and, thus, the above-mentioned three different decaying processes occur [10]. The overall enhancement of the fluorescence intensity observed after glucose addition has been ascribed to the increase of contribution of the fluorescence process characterized by intermediate lifetime (τ_I) that results from the change of the equilibrium between open and closed conformations caused by the chemical reduction of FAD to $FADH_2$. This hypothesis has been confirmed by the observation of a fluorescence quenching of the fast and long components. Moreover we have shown that some parameters coming from fluorescence decay curve analysis are strongly sensitive to the glucose concentration and feature a Michaelis-Menten type behaviour [10]. These characteristics make time-resolved fluorescence spectroscopy very promising for glucose sensing by using GOD-based optical devices with particular attention to sol–gel immobilized enzyme. In fact sol–gel technology has a predominant role in preparing bioactive materials for optical biosensing owing to its high versatility allowing the manipulation of the material characteristics required for particular applications [10, 18–20].

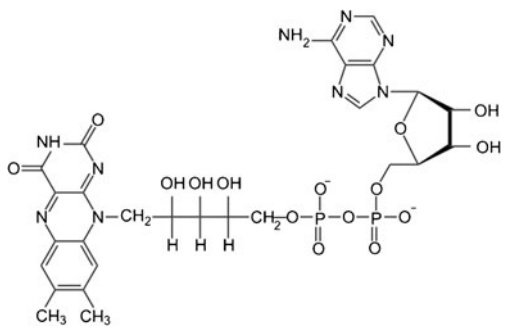

Fig. 1 Structural formula of flavin adenine dinucleotide (FAD)

The aim of the present paper is to further extend the time-resolved fluorescence spectroscopy investigation of FAD emission in the time interval immediately following the addition of glucose in order to study the interaction between sol–gel immobilized GOD and glucose. Given the dependence of GOD fluorescence characteristics on glucose concentration, experiments have been carried out on immobilized GOD interacting with glucose at various concentrations, one (2 mM) in the linear region of the Michaelis-Menten curve and two (10 mM and 15 mM) in the saturation region. The decay curves have been analysed using the three-exponential model [10]. This approach has allowed us to detect the FAD conformational changes occurring during the immobilized GOD-glucose interaction and to outline a change from a configuration with a prevalent role of the state characterized by the long lifetime to a configuration with increased contribution from the process with the intermediate lifetime. The time needed to complete this configuration change is dependent on the added glucose concentration and spans from some hundreds of seconds (at c=2 mM) down to 100 s or less (at c= 15 mM). It is worthwhile to note that these results can give an important contribution in understanding the mechanisms involved in solid state biocatalysis, which are fundamental for biotechnological applications.

Materials and Methods

Materials

All chemicals were purchased from Sigma (Sigma Italia, Milan, Italy), with the exception of tetramethoxysilane (TMOS) and glucose oxidase (GOD), which were purchased from Fluka (Fluka Italia, Milan, Italy). In this study glucose oxidase (GOD, EC 1.1.3.4) from Aspergillus niger (154 U mg^{-1}) was used.

Methods

Preparation of the Catalytic Sol–Gel Matrices

Sol–gel matrices have been proven to be excellent carriers for enzymes since their catalytic activity is slightly affected

by the gel structure. In addition sol–gel avoids the leakage of the bioactive macromolecule and allows the diffusion of substrate (and reaction products) towards (or away from) the catalytic site [20–23]. For the present series of measurements silica gel matrices were prepared, as described in a previous paper [24], by rapid mixing 800 μL of solution A with 800 μL of solution B in a polymethylmethacrylate cell. Solution A was obtained by slowly mixing (for 1 h at 4 °C) TMOS (1,550 μL) with H_2O (450 μL) plus 40 mM HCl (30 μL). Solution B contained 0.1 M phosphate buffer at pH 6.5. The A and B solution mixture (1,600 μL) was poured into a polymethylmethacrylate cell that was sealed with paraffin film and placed horizontally until the gel was formed. To avoid cracking in the formed gel, the cell was filled with 0.1 M phosphate buffer at pH 6.5 and stored overnight in a refrigerator at 4 °C. The day after, the silica gel layer was removed from the cell and was ready for use. The catalytic gel was obtained with solution B containing an additional 20 mg/mL of GOD in 0.1 M phosphate buffer at pH 6.5.

In order to study the effects of the immobilization procedure on GOD optical properties, GOD absorption and fluorescence emission spectra were recorded before and after the completion of the procedure by using a Lambda 25 Perkin-Elmer spectrophotometer and a LS55 Perkin-Elmer spectrofluorimeter, respectively (details in Reference [25]). Absorption and fluorescence emission spectra of GOD free and entrapped in the sol–gel matrix are shown in Fig. 2. As for the absorption, spectra from free and immobilized GOD (Fig. 2a) display three peaks at 275 nm, and at about 380 and 450 nm. Steady state fluorescence emission spectra (following an excitation at 450 nm) from free and immobilized GOD (Fig. 2b) feature a maximum at about 530 nm, due to FAD intrinsic fluorescence. The evidence that absorption and fluorescence spectra of free and immobilized GOD have similar characteristics is in agreement with reported data [26] showing that sol–gel immobilization prevents alterations in GOD optical properties.

The entrapment of GOD in silica gel changes the properties of the enzyme because of the interactions of the molecule with silica surface inside the pores and different microenvironment [20, 27–29]. The change in its conformation leads to a restriction of the molecule motion and lower accessibility of the entrapped enzyme by the substrate [23]. This lower accessibility is of fundamental importance in the present investigation since modulates the GOD-glucose interaction on a time scale accessible to our experimental technique. The properties of GOD immobilized in the proposed silica gel were extensively investigated in Reference [24] where an apparent value of Michaelis–Menten constant larger than that obtained for free GOD was obtained as a result of its lower activity together with a high catalytic stability. All the measurements were performed at room temperature.

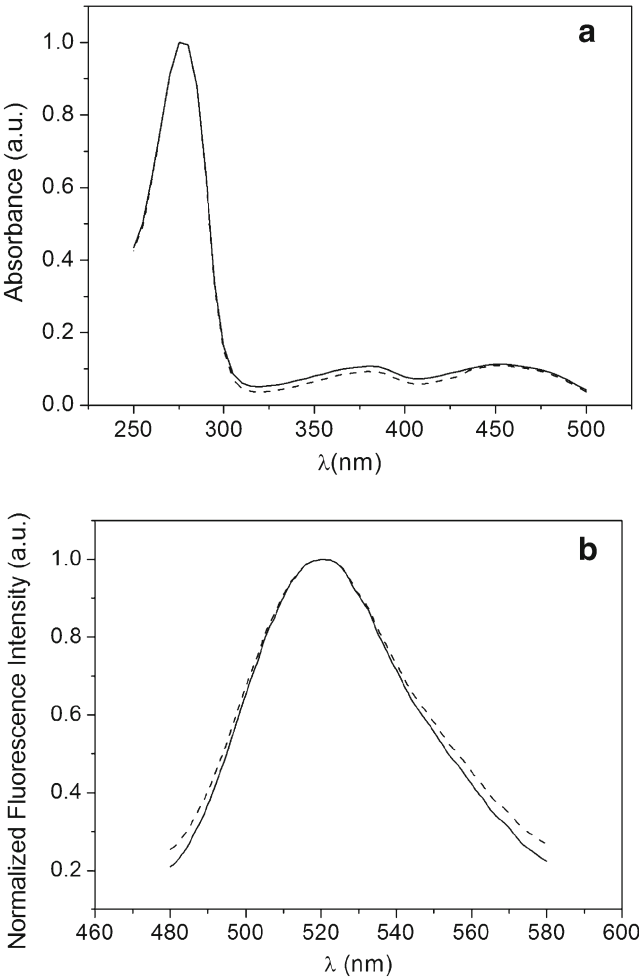

Fig. 2 **a** Absorption spectra of free (——) and immobilized (- - - -) GOD. **b** Steady state fluorescence emission spectra of free (——) and immobilized (- - - -) GOD in the visible range. Samples were excited at 450 nm and emission spectra were considered between 500 and 580 nm. (For details, see Reference [25])

Time-Resolved Fluorescence Measurements

In time-resolved fluorescence experiments sample excitation was provided by a picosecond diode laser emitting pulses at a repetition rate of 40 MHz and a wavelength of 405 nm, close to the absorption maximum of the first electronic transition of the bound flavin [10]. The laser beam was focused into a 10 mm sample cell by a microscope objective lens. The fluorescence emission was detected at 90° to the incident light beam to minimize the amount of transmitted or reflected beam light reaching the detector. A bandpass filter blocks the residual laser beam and allows only radiation with a wavelength of 520±10 nm to reach the detector, the chosen wavelength range being close to the maximum of GOD fluorescence emission spectrum. The detection apparatus was composed of a fast multichannel plate photomultiplier tube and a time-correlated single-photon counting (TCSPC) electronics.

The instrument response function (IRF) determined by TCSPS was about 120 ps FWHM. See Reference [10] for further details.

Changes in fluorescence decay caused by the enzymatic reaction upon the addition of different glucose concentrations were detected and monitored every 20 s with acquisition time of 20 s until the reaction cycle between GOD and glucose takes place. Analysis of fluorescence transients was performed through a fitting procedure with a three-exponential model, in agreement with the description of redox reaction proposed in References [8, 9]. Effects of the system response were taken into account by convolving the analytical model with IRF, according to the following expression [10]:

$$I(t) = IRF(t) \otimes \sum_{i=S,I}^{L} \frac{\alpha_i}{\tau_i} \exp\left(-\frac{t}{\tau_i}\right) \quad (1)$$

where the pre-exponential factor α_i is the total fluorescence intensity for the i-th emitting component with lifetime τ_i (i = S, I, L for indicating short-, intermediate-, and long-lifetime process, respectively). The mean lifetime τ_M is obtained by the classical relationship:

$$\tau_M = \frac{\sum \alpha_i \tau_i}{\sum \alpha_i} = \sum f_i \tau_i \quad (2)$$

where f_i are the fractional steady-state intensities of each lifetime component:

$$f_i = \frac{\alpha_i}{\sum \alpha_i} \quad (3)$$

Results and Discussion

Figure 3 shows the fluorescence decay curves as detected from GOD immobilized in a sol–gel layer prior (black line) and after the addition of glucose at 2 mM (red circles), 10 mM (green squares) and 15 mM (blue triangles) concentration. It can be clearly seen that the inclusion of glucose induces an increase in the fluorescence peak value with a corresponding increase of the integral area under the spectrum. This is in agreement with previous findings [9, 10, 24, 30, 31] showing that the presence of proper amount of glucose in solution has the effect of enhancing GOD fluorescence intensity. The three-exponential model has been used for fitting the experimental curves; accordingly Eq. 1 has been used as analytical model. The estimated parameters are shown in Table 1. The inspection of the resulting total intensity shows that it increases with glucose concentration, thus confirming the effect of fluorescence intensity enhancement, which lasts until the reaction cycle between GOD and glucose takes places, as it has been previously shown [8, 10]. Additionally, fractional steady-state intensity parameters indicate that the dominant configuration of the protein is the open one characterized by a long lifetime for all the samples. As concerns the lifetimes, no comments can be done on the shortest one (τ_S) because it is below the time resolution of our apparatus, the long lifetime (τ_L) is quite constant within the errors, while the intermediate lifetime (τ_I) is around 350 ps in absence and in presence of glucose at the highest concentration and decreases to around 150 ps for the other two examined samples (glucose at 5 and 10 mM). The mean lifetime (τ_M) shows a general decrease with increasing glucose concentration.

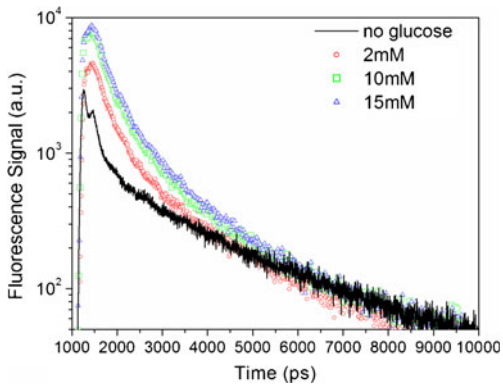

Fig. 3 Fluorescence signal for immobilized GOD when excited in the FAD region (λ_{exc}=405 nm) without (*black continuous line*) and with glucose (2 mM–*red circles*, 10 mM–*green squares*, and 15 mM–*blue triangles*)

Figure 4 shows the values of the integral area under the fluorescence decay curve as a function of the reaction time for the three glucose concentrations. For all of the glucose concentrations an increase in the total fluorescence intensity is detected confirming the results obtained using a time coarse measurement at various glucose concentrations [30, 31]. Instead, the temporal behaviour of the signal depends on glucose concentration. For glucose at 2 mM and 10 mM concentrations the total fluorescence intensity initially remains constant and after some time (longer for the low concentration than for the high one) it increases gradually to a maximum value and then tends to gradually decrease. The maximum value of the integrated intensity is almost the same for the two concentrations, resulting around 1.5, but it is reached around 600 s after glucose addition for the 2 mM sample and after less than 200 s when there are more glucose molecules available for the interaction with GOD (hence, when glucose is at 10 mM concentration). The temporal behaviour of the signal outlined when glucose at 15 mM concentration is added is slightly different, the initial region of constant value lacking. In this case the total fluorescence intensity begins to increase immediately after glucose addition and reaches its maximum value within 100 s. After this time a slow decrease occurs. From these results it seems that the higher the glucose concentration the

Table 1 Parameters (total fluorescence intensity, lifetimes τ_I, mean lifetime τ_M and relative amplitude f_i) as obtained by fitting the experimental GOD time-resolved fluorescence signal with the three-exponential model (see text) for sol–gel immobilized GOD in absence and in presence of glucose at various concentrations

Fitting parameters	GOD	GOD + 2 mM glucose	GOD + 10 mM glucose	GOD + 15 mM glucose
Total intensity (a.u.)	0.574	1.156	1.257	1.366
f_S	0.14±0.01	0.10±0.01	0.15±0.01	0.23±0.02
f_I	0.16±0.01	0.13±0.01	0.17±0.01	0.15±0.01
f_L	0.70±0.06	0.77±0.06	0.68±0.07	0.62±0.06
τ_S (ps)	8±3	3±1	6±2	12±2
τ_I (ps)	380±70	158±19	155±18	317±25
τ_L(ps)	2960±190	2260±50	2450±60	2070±60
τ_M (ps)	2126	1755	1698	1325

faster the signal increase and the amount of the variation are. It is important to note that the behaviour of the curves shown in Fig. 4 is strongly influenced by the presence of the sol–gel matrix. In fact time coarse measurements [31] have already demonstrated that immobilized enzyme reacts with glucose more slowly due to diffusion effects. Sol–gel can modulate the diffusion processes depending on its physico-chemical properties, as different pore sizes [27].

To get a better insight into the interaction between sol–gel immobilized GOD and glucose the fluorescence decay curves at various reaction times have been analysed by the three-exponential model.

In Fig. 5 the temporal behaviour of f_S, f_I and f_L for the samples at the three investigated glucose concentrations (2 mM, 10 mM and 15 mM) is reported in the a, b and c panel, respectively. As is clearly evident the f_S component dependence on the reaction time is different for the various glucose concentrations. At 2 mM glucose concentration f_S has its highest value (about 0.15) at short reaction times and

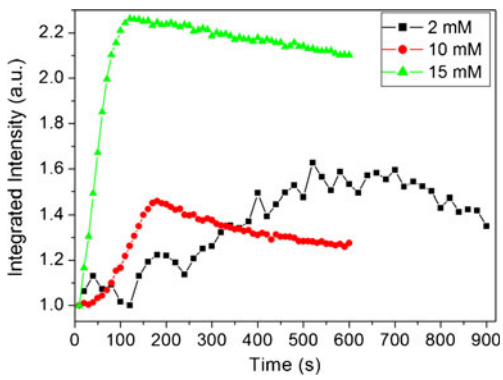

Fig. 4 Normalized fluorescence total intensity as a function of time during the enzymatic reaction of the GOD entrapped in the sol gel matrix. The data have been normalized to the value observed at t=0. Curves are for samples with added glucose (**a**) and with added glucose at (**b**) 2 mM, (**c**) 10 mM and (**d**) 15 mM concentration in 0.1 M phosphate buffer, pH=6.5

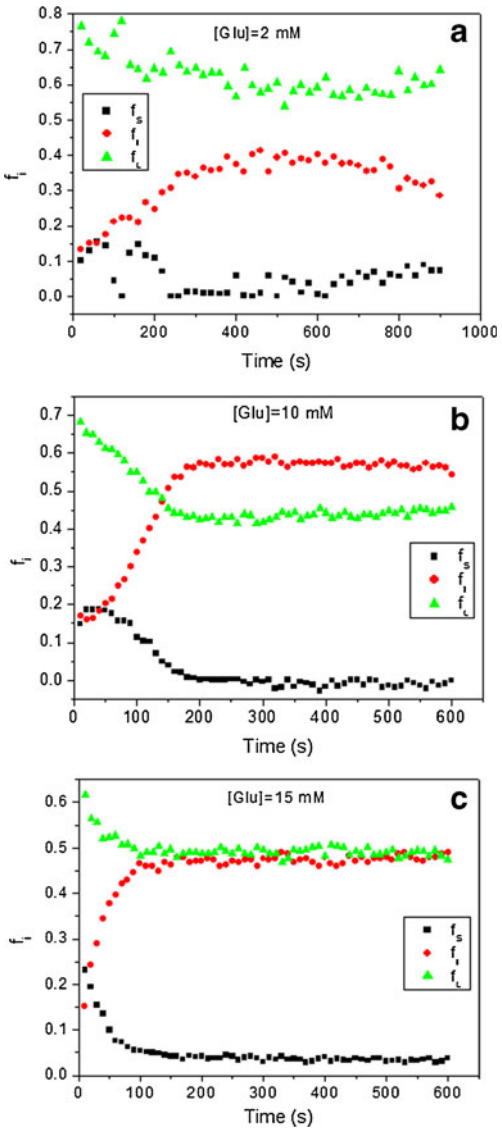

Fig. 5 f_i values as obtained from the fitting procedure for 2 mM (panel **a**), 10 mM (panel **b**), 15 mM (panel **c**) glucose concentration in 0.1 M phosphate buffer, pH=6.5. Fitting errors within a few percents

slightly decreases, becoming negligible. After 450 s from glucose addition it begins to slightly increase toward a constant value. However, these variations are very small and are difficult to be quantitatively evaluated. At a glucose concentration of 10 mM, f_S maintains a constant value (0.2) at short times, beginning a linear decrease 80 s after glucose has been added. The decrease ceases at about 180 s after glucose addition when a negligible value is reached. At the highest glucose concentration (15 mM), f_S rapidly decreases from its maximum value (0.2 at 0-s reaction time) to a constant value (0.05), never reaching negligible values in the investigated reaction time interval. On the contrary, the dependence of f_I and f_L on the reaction time seems to be not influenced by glucose concentration. In fact, in all the three cases f_I has a value of around 0.15 at 0-s reaction time and increases until a constant value (f_I*) is reached. However, both the time (T_{fI}) needed for reaching the constant value and f_I* itself depend on glucose concentration. In particular, T_{fI} monotonously decreases with glucose concentration from 400 s (at 2 mM) to 100 s (at 15 mM), resulting 200 s at 10 mM glucose concentration. f_I* is 0.4, 0.55 and 0.45 at 2 mM, 10 mM and 15 mM glucose concentration, respectively. Conversely f_L always shows an initial decrease from a maximum value (resulting to be around 0.8, 0.7 and 0.65 at 2 mM, 10 mM and 15 mM glucose concentration, respectively) which ceases when a constant value (f_L*) is reached. f_L* is 0.6, 0.45 and 0.45 at 2 mM, 10 mM and 15 mM glucose concentration, respectively. The f_L decrease lasts about 220 s at 2 mM glucose concentration, 170 s at 10 mM and 120 s at 15 mM. Hence, naming this time as T_{fL}, T_{fL} decreases monotonously with glucose concentration like T_{fI} does.

The analysis of these results in terms of GOD conformation suggests that immediately after glucose addition sol–gel immobilized GOD is mainly (70–80 %, as indicated by f_L values around 0.7–0.8) in the open conformation (corresponding to the slowly decaying component) and the rest is equally divided in the closed (fast component) and intermediate conformation. After a period (T_{fI} and T_{fL}, depending on the process) in which the relative content of the two conformations (giving rise to an ensemble overall conformation) changes monotonously, an equilibrium ensemble configuration seems to be envisaged as occurring at the end of the investigated reaction time. The equilibrium configuration is dependent on glucose concentration. In fact, when a low number of glucose molecules (glucose at 2 mM concentration) is available for the interaction, 60 % of GOD is still in the open conformation, 30 % is in the intermediate one and 10 % is in the closed conformation, the open conformation having been the most frequent one during all the investigated time. On the contrary, the number of GOD molecules which are thought to be in the intermediate conformation overcomes the number of those in the open one after the reaction with glucose at 10 mM (55 % featuring an intermediate conformation and 45 % a open one); no GOD molecules resulting to be in closed conformation at the end of the investigated period of reaction. At the highest glucose concentration, 45 % of GOD molecules is in open conformation, 45 % in the intermediate one, and 10 % in closed conformation at the end of the investigated reaction time. As for the characteristic time of the transition between the initial ensemble conformation of the enzyme and the one envisaged at the end of the investigated interaction time, in both the cases the time for reaching the final configuration (T_{fI} and T_{fL}) monotonously decreases with glucose concentration, suggesting that the higher the glucose concentration the faster the reaction between GOD and glucose is.

The values obtained from the three-exponential model analysis for short, intermediate and long lifetimes are shown in Fig. 6 as a function of the reaction time for all the investigated glucose concentrations. The values of τ_S are always lower than the experimental time resolution and hence they are not considered for the discussion. The intermediate lifetime (τ_I) shows the same dependence on the reaction time for all the three glucose concentrations: τ_I increases with time until $T_{\tau I}$, when a constant value (τ_I*) is reached. $T_{\tau I}$ values range from around 20–30 s to 300 s, the smallest value having been obtained with glucose at 15 mM and the largest at 2 mM. For the sample at 10 mM glucose concentration $T_{\tau I}$ is around 150 s. As far as the τ_I* values, the smallest one (about 340 ps) is obtained at 2 mM glucose concentration. At 10 mM and 15 mM a value around 400 ps is obtained. Also τ_L parameter shows the same dependence on the reaction time for all the three glucose concentrations. In particular, τ_I decreases almost linearly from a maximum value (τ_L^m) to a constant value (τ_L*); the τ_L* value is reached after a time $T_{\tau L}$. The extracted τ_L^m values are around 2.4 ns, 2.5 ns and 2.1 ns at 2 mM, 10 mM and 15 mM glucose concentration, respectively. The observed τ_L* values are around 1.9 ns, 2.1 ns and 1.8 ns for glucose at 2 mM, 10 mM and 15 mM concentration, respectively. The time needed to the long lifetime to reach the constant value has a clear monotonous dependence on glucose concentration, showing a significant decrease with glucose content. In fact, the highest value (about 550 s) is obtained at 2 mM glucose concentration while $T_{\tau L}$ is around 250 s at 10 mM and 100 s at 15 mM. It's worth mentioning that τ_I*, τ_L^m, τ_L* values are quite constant, within 10 % of the single values, over the investigated glucose concentrations. On the contrary, the times needed for reaching the final characteristic times (namely, $T_{\tau I}$ and $T_{\tau L}$) monotonously decrease with glucose concentration, confirming that the presence of a higher number of glucose

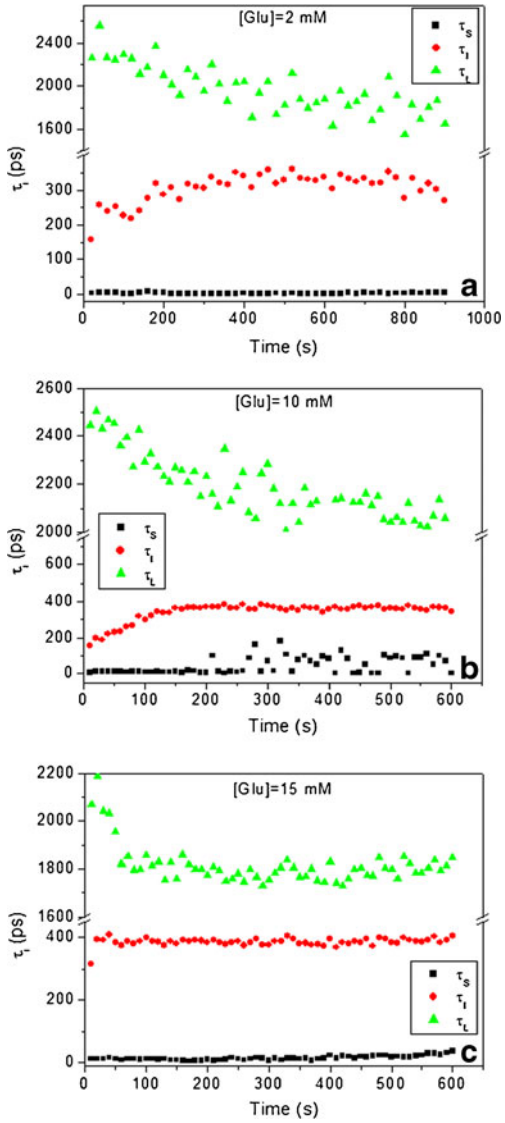

Fig. 6 τ_i values as obtained from the fitting procedure for 2 mM (panel **a**), 10 mM (panel **b**), 15 mM (panel **c**) glucose concentration in 0.1 M phosphate buffer, pH=6.5. Fitting errors within a few percents

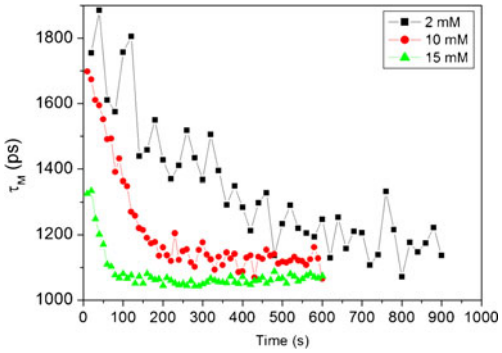

Fig. 7 Mean lifetime, $\tau(\tau_M)$, for 2 mM, 10 mM, 15 mM glucose concentration in 0.1 M phosphate buffer, pH=6.5. Fitting errors within a few percents

molecules makes faster reaching the equilibrium configuration in a cycle.

The overall dependence of the lifetimes on both reaction time and glucose concentration can be understood by analysing the values of τ_M, as obtained using Eq. 2, shown in Fig. 7 as a function of the reaction time. By inspecting that figure, it comes out that whatever the concentration is, τ_M monotonously decreases from a maximum value (τ_M^m), featured immediately after glucose addition, to a constant one (τ_M*) which is reached after a time ($T_{\tau M}$). The value detected for the mean lifetime at the end of the reaction, i.e. τ_M*, is around 1.1 ns for all the concentrations. Noteworthy, both τ_M^m and $T_{\tau M}$ decrease with glucose concentration. In fact, τ_M^m is 1.8 ns, 1.7 ns and 1.3 ns for a glucose concentration at 2 mM, 10 mM and 15 mM, respectively. $T_{\tau M}$ ranges from the greatest value (800 s) obtained at 2 mM down to 120 s when glucose concentration is at 15 mM. For the intermediate value of glucose concentration (10 mM) $T_{\tau M}$ is 250 s. Since the value of the mean lifetime reflects both the relative percentage of the single decaying processes and their characteristic times, these evidences further confirm that the presence of a higher number of glucose molecule makes faster reaching the equilibrium configuration in an interaction cycle.

In summary, the results here discussed allow us to say that the interaction between GOD and glucose induces a change in conformation from a configuration with a prevalent role of the state characterized by the long lifetime to an equilibrium configuration with increased contribution from the process with the intermediate lifetime. Additionally, inspecting all the fluorescence decay parameters, it is possible to extract the order of magnitude of the time needed to reach this equilibrium configuration. In particular, at c= 2 mM the equilibrium configuration is reached within some hundreds of seconds (T_{fI} = 400 s, T_{fL} = 220 s, $T_{\tau I}$ = 300 s, $T_{\tau L}$ = 550 s, $T_{\tau M}$ = 800 s), at c=10 mM the time needed to reach the final configuration seems to be about 200 s (T_{fI} = 200 s, T_{fL} = 170 s, $T_{\tau I}$ = 150 s, $T_{\tau L}$ = 250 s, $T_{\tau M}$ = 250 s), at c = 15 mM it is 100 s or less (T_{fI} = 100 s, T_{fL} = 120 s, $T_{\tau I}$ = 20–30 s, $T_{\tau L}$ = 100 s, $T_{\tau M}$ = 120 s).

All these results indicate that there is a significant dependence of the analyzed parameters on glucose concentration. This behaviour has been ascribed to the kinetics of the process, in particular to the reoxidation of $FADH_2$. The reoxidation process proceeds at a constant rate greater than that at which the solution takes up O_2 from the surrounding atmosphere (mass transfer). Initially, the reaction involves a net uptake of O_2, since the mass transfer rate is very low and catalysis produces only one-half of the oxygen consumed. As the reaction proceeds, the glucose concentration and the O_2 uptake decrease. The mass transfer rate becomes significant and eventually equals the oxygen uptake rate, so a steady

state is reached, after which the mass transfer rate exceeds the uptake rate, and the concentration of dissolved O_2 increases gradually. While the oxidation kinetics of $FADH_2$ exceeds its production rate, the predominant species will be FAD and the fluorescence intensity remains constant at the beginning. As the concentration of dissolved O_2 decreases, so it does the rate of FAD regeneration. Below a given level, $FADH_2$ becomes the predominant species and the fluorescence intensity increases. The opposite process takes place when the concentration of O_2 starts to rise again by mass transfer. As said before the temporal behaviour of the process is strongly influenced by the presence of the sol–gel matrix since sol–gel can modulate the diffusion processes depending on its physico-chemical properties, as different pore sizes.

Conclusions

In the present paper time-resolved fluorescence spectroscopy was used to monitor FAD signals from sol–gel immobilized GOD in the time interval immediately following the addition of glucose in order to deeper investigate GOD-glucose interaction. Analysing the experimental decay curves in terms of a three-exponential model allowed us to detect the FAD conformational changes occurring during the interaction. In particular, the analysis of recorded decay curves showed that the FAD conformational state changes from a configuration with a prevalent role of the state characterized by the long lifetime to an equilibrium configuration with increased contribution from the process with the intermediate lifetime. Additionally, the characteristic times of the interaction and their dependence on glucose concentration were obtained, featuring that the presence of a higher number of glucose molecule makes faster reaching the equilibrium configuration. The time to reach equilibrium spans from some hundreds of seconds (at c=2 mM) down to 100 s or less (at c=15 mM).

On one hand these results confirm the potentials of time-resolved fluorescence in better understanding the interaction between immobilized proteins and substrates during enzymatic reactions and in characterizing immobilized enzymes. More importantly, they provide additional information on the specific interaction between sol–gel immobilized GOD and glucose, which would increase the affordability of the description of the interaction, a goal of great importance from the fundamental standpoint. These advances deserves particular interest also for applications because they deal with immobilized GOD. In fact, a better knowledge of the internal conformation immobilized GOD when participating to GOD-glucose interaction and of the characteristic times of the conformation transition would help in defining immobilization strategies or in designing new glucose GOD-based biosensors.

Acknowledgments The authors are pleased to acknowledge B. Della Ventura for his valuable contribution to experimental procedures.

References

1. Steiner MS, Duerkop A, Wolfbeis OS (2011) Optical methods for sensing glucose. Chem Soc Rev 40:4805–4839
2. McShane MJ (2002) Potential for glucose monitoring with nanoengineered fluorescent biosensors. Diabet Technol Therap 4:533–538
3. Brown JQ, Srivastava R, Zhu H, McShane MJ (2006) Enzymatic fluorescent microsphere glucose sensors: evaluation of response under dynamic conditions. Diabet Technol Therap 8:288–295
4. Singh K, Singh BP, Chauhan R, Basu T (2012) Fabrication of amperometric bienzymatic glucose biosensor based on MWCNT tube and polypyrrole multilayered nanocomposite. J Appl Polym Sci 125:E235–E246
5. Ferri S, Kojima K, Sode K (2011) Review of glucose oxidases and glucose dehydrogenases: a bird's eye view of glucose sensing enzymes. J Diabetes Sci Tech 5:1068–1076
6. Pickup JC, Hussain F, Evans ND, Rolinski OJ, Birch DJS (2005) Fluorescence-based glucose sensors. Biosens Bioelectron 20:2555–2565
7. Haouz A, Twist C, Zentz C, Tauc P, Alpert B (1998) Dynamic and structural properties of glucose oxidase enzyme. Eur Biophys J 27:19–25
8. Trettnak W, Wolfbeis OS (1989) Fully reversible fibre-optic glucose biosensor based on the intrinsic fluorescence of glucose oxidase. Anal Chim Acta 211:195–203
9. Lepore M, Portaccio M, De Tommasi E, De Luca P, Bencivenga U, Maiuri P, Mita DG (2004) Glucose concentration determination by means of fluorescence emission spectra of soluble and insoluble glucose oxidase: some useful indications for optical fibre-based sensors. J Mol Catal B Enzym 31:151–158
10. Esposito R, Della Ventura B, De Nicola S, Altucci C, Velotta R, Mita DG, Lepore M (2011) Glucose sensing based on the intrinsic time-resolved visible fluorescence of sol–gel immobilized glucose oxidase. Sensors 11:3483–3497
11. James TL, Edmondson DE, Husain M (1981) Glucose oxidase contains a disubstituted phosphorus residue. Phosphorus-31 nuclear magnetic resonance studies of the flavin and nonflavin phosphate residues. Biochemistry 20:617–621
12. Mitra C, Torstensson A (1980) Spectroscopic, NMR, and theoretical studies on the intramolecular electron transfer in FAD. J Electroanal Chem Interf Electrochem 116:749–756
13. Wille G, Ritter M, Friedemenn R, Mäntele W, Hubner G (2003) Redox-triggered FTIR difference spectra of FAD in aqueous solution and bound to flavoproteins. Biochemistry 42:14814–14821
14. Fujiwara A, Mizutani Y (2008) Photoinduced electron transfer in glucose oxidase: a picosecond time-resolved ultraviolet resonance Raman study. J Raman Spectrosc 39:1600–1605
15. Stanley R, MacFarlane A (2000) Ultrafast excited state dynamics of oxidized flavins: direct observations of quenching by purines. J Phys Chem A 104:6899–6906
16. van den Berg P, Feenstra K, Mark A, Berendsen H, Visser A (2002) Dynamic conformations of flavin adenine dinucleotide: simulated molecular dynamics of the flavin cofactor related to the time-resolved fluorescence characteristics. J Phys Chem B 106:8858–8869

17. Zhong D, Zewail AH (2001) Femtosecond dynamics of flavoproteins: charge separation and recombination in riboflavine (vitamin B2)-binding protein and in glucose oxidase enzyme. Proc Natl Acad Sci U S A 98:11867–11872
18. Jeronimo PCA, Araujo AN, Montenegro MCBSM (2007) Optical sensors and biosensors based on sol–gel films. Talanta 72:13–27
19. Wolfbeis OS, Oehme I, Papkovskaya N, Klimant I (2000) Sol–gel based glucose biosensors employing optical oxygen transducers, and a method for compensating for variable oxygen background. Biosens Bioelectron 15:69–76
20. Przybyt M, Miller E, Szreder T (2011) Thermostability of glucose oxidase in silica gel obtained by sol–gel method and in solution studied by fluorimetric method. J Photochem Photobiol B Biol 103:22–28
21. Pierre AC (2004) The sol–gel encapsulation of enzymes. Biocatal Biotransform 22:145–170
22. Mac Craith B, Mc Donagh C, McEvoy A, Butler T, O'Keeffe G, Murphy V (1997) Optical chemical sensors based on sol–gel materials: recent advances and critical issues. J Sol–gel Sci Technol 8:1053–1061
23. Jin W, Brennan JD (2002) Properties and applications of proteins encapsulated within sol–gel derived materials. Anal Chim Acta 461:1–36
24. Portaccio M, Lepore M, Della Ventura B, Stoilova O, Manolova N, Rashkov I, Mita DG (2009) Fiber-optic glucose biosensor based on glucose oxidase immobilised in a silica gel matrix. J Sol–gel Sci Technol 50:437–448
25. Delfino I, Portaccio M, De Rosa M, Lepore M (2013) A preliminary investigation on the interaction between sol–gel immobilized glucose oxidase and freely diffusing glucose by means of two-photon microscopy. Proc SPIE 8588:85882U/1-12
26. Qingwen L, Guoan L, Yiming W, Xingrong Z (2000) Immobilization of glucose oxidase in sol–gel matrix and its application to fabricate chemiluminescent glucose sensor. Mater Sci Eng C 11:67–70. doi:10.1016/S0928-4931(00)00130-2
27. Chaudhury NK, Chandra S, Mathew TL (2001) Oncologic applications of biophotonics: prospects and problems. Appl Biochem Biotechnol 96:183–204
28. Gupta R, Kumar A (2008) Bioactive materials for biomedical applications using sol–gel technology. Biomed Mater 3:034005. doi:10.1088/1748-6041/3/3/034005
29. Delfino I, Portaccio M, Della Ventura B, Mita DG, Lepore M (2013) Enzyme distribution and secondary structure of sol–gel immobilized glucose oxidase by means of micro-attenuated total reflection FT-IR spectroscopy. Mater Sci Eng C 33:304–310. doi:10.1016/j.msec.2012.08.044
30. Sierra JF, Galban J, Castillo JR (1997) Determination of glucose in blood based on the intrinsic fluorescence of glucose oxidase. Anal Chem 69:1471–1476
31. De Luca P, Lepore M, Portaccio M, Esposito R, Rossi S, Bencivenga U, Mita DG (2007) Glucose determination by means of steady-state and time-course UV fluorescence in free or immobilized glucose oxidase. Sensors 7:2612–2625